

T Tauri stars and the Gould Belt near Lupus[★]

R. Wichmann¹, M. Sterzik², J. Krautter², A. Metanomski^{1,3}, and W. Voges²

¹ Landessternwarte Königstuhl, D-69117 Heidelberg, Germany

² Max-Planck-Institut für Extraterrestrische Physik, D-85740 Garching, Germany

³ European Southern Observatory, La Silla, Chile

Received 2 December 1996 / Accepted 29 January 1997

Abstract. We present results of a study to investigate the spatial distribution of X-ray active young stellar objects near the Lupus star forming region (SFR). In this SFR, a recent study has led to the discovery of some 130 new *weak-line T Tauri stars* (WTTS) dispersed over a large area of some 230 square degrees. However, the true extent of the spatial distribution of these stars could not be determined in this study.

We have selected from the ROSAT All-Sky-Survey candidate T Tauri stars within a narrow strip of 10° width, located adjacent to the Lupus SFR, and oriented perpendicular to the galactic plane. Intermediate resolution spectroscopy was carried out to identify stellar objects with strong Li I $\lambda 6708$ absorption, indicative of their youth, and 48 Li-rich stars were found within our study region.

The peak at $b \simeq 18^\circ$ in the spatial distribution of Li-rich stars within this strip corresponds well with the intersection of our study region with the Gould Belt, but is inconsistent with the assumption that these stars belong to a galactic ZAMS foreground population, which would be expected to be centered on the galactic midplane.

We conclude that the majority of recently discovered low-mass, X-ray active, Li-rich stars dispersed over large areas around Gould Belt SFRs are indeed WTTS with ages not exceeding that of the Gould Belt itself, i.e. below $5 - 6 \times 10^7$ years.

Key words: stars: formation – stars: late-type – stars: pre-main sequence – X-rays: stars

1. Introduction

Using data from the ROSAT All Sky Survey (RASS), in a recent study Krautter et al. (1997) have addressed the problem of the large-scale spatial distribution of pre-main sequence (PMS)

Send offprint requests to: R. Wichmann

[★] Based on observations collected at European Southern Observatory, Chile (observing proposals ESO N^o 57.E-0721).

stars in the Lupus star forming region (SFR). The exciting result of this study was that the population of X-ray selected weak-line T Tauri stars (WTTS) extends far beyond the regions of star forming molecular clouds, where the optically selected T Tauri stars (TTS) - mainly classical T Tauri stars (CTTS) - are located. This result is in line with similar studies of other SFRs (cf. Wichmann et al. 1996, Alcalá et al. 1995, Sterzik et al. 1995, Neuhäuser et al. 1995), where also many widely dispersed WTTS have been found.

The origin of these dispersed WTTS is not clear yet, and different explanations have been suggested. They could have formed in the star forming clouds and afterwards been dispersed by the velocity dispersion of a few km/s typical for SFRs (Jones & Herbig 1979, Dubath et al. 1996) as suggested by Wichmann et al. (1996), they could have been ejected from the clouds by a gravitational 'slingshot' mechanism discussed by Sterzik & Durisen (1995), or they could have formed in outlying small turbulent cloudlets as proposed by Feigelson (1996). Alternatively, these WTTS might also represent zero-age main sequence (ZAMS) stars of about 10^8 yrs rather than PMS stars of some $10^6 - 10^7$ yrs (Briceño et al. 1997).

However, some information on the origin of the dispersed WTTS can be inferred from their spatial distribution. The Lupus SFR is part of a well-known local structure in the Galaxy first described in some detail by Gould (1879), and therefore named the Gould Belt. It is a ring-like expanding structure of some 800–1000 pc diameter, inclined some 20° with respect to the Galactic Plane and outlined by OB stars, molecular gas, and nearby SFRs (like Lupus, Orion, and Chamaeleon). The Sun is located in the plane of this structure, but some 150–200 pc off-center. The origin of the Gould Belt is not known, but since it is expanding, some violent event like the impact of a high-velocity cloud on the Galactic Plane or an explosive event near its center seems to have caused this structure. For a short history of the investigation of the Gould Belt see Stothers & Frogel (1974).

The stellar population of the Gould Belt suggests an age of about $5 - 6 \times 10^7$ yrs (Comerón et al. 1994, Westin 1985). Estimated expansion ages, which are more model-dependent, range from $3 - 7 \times 10^7$ yrs (Olano 1982, Westin 1985, Frogel & Stothers 1977, Comerón & Torra 1990, Pöppel et al. 1994).

Thus the Gould Belt is significantly younger than 10^8 yrs, and late-type stars which can be shown to belong to this structure are most probably still in the PMS stage of their evolution.

If the dispersed WTTS found near the Lupus SFR are ZAMS stars with an age of about 10^8 yrs that are completely unrelated to the Lupus SFR, as proposed by Briceño et al. (1997), then their spatial distribution would correlate not with the (younger) Gould Belt, but most likely with the Galactic Plane. On the other hand, if it can be shown that their spatial distribution correlates with the Gould Belt, we can presume that they are members of the Gould Belt, have ages not exceeding that of the Gould Belt, and that they are related to the Lupus SFR, which is of the Gould Belt. This would be an independent confirmation of the conclusions of Krautter et al. (1997) and Wichmann et al. (1996), namely that these dispersed WTTS are PMS stars with an age of a few 10^7 yrs.

The survey of Krautter et al. (1997) covered a large area of some 230 square degree which, however, was not sufficient to determine the extent of the spatial distribution of the WTTS found by them. Therefore, we chose to study RASS X-ray sources in a narrow strip on the sky, oriented perpendicular to the Galactic Plane, in order to identify new WTTS and to investigate their spatial distribution. This strip was 10° wide, centered on $l = 330^\circ$, and extended from $b = -5^\circ$ to $b = 50^\circ$. It thus crosses the region studied by Krautter et al. (1997), but does not include the Lupus dark clouds, where the classical TTS of the Lupus SFR are located.

2. Source selection

Of the 1001 RASS sources in our study area, only about 20% can be identified with known stellar and extragalactic counterparts in the Simbad database. Clearly, for efficient ground-based optical follow-up observations a pre-selection among the remaining sample of more than 800 X-ray sources is needed. A general statistical discrimination method was introduced by Sterzik et al. (1995) in order to find promising TTS candidates in the ROSAT database and was applied to study the spatial distribution of TTS candidates in the Orion SFR. In the present case, we apply the same method to our sample of RASS sources. A detailed description of the procedure can be found in Sterzik et al. (1995), here we only summarize the relevant steps:

1. We establish a “training-set”, consisting of members of previously classified groups, in our case TTS and non-TTS. The training set we used is described in detail in Sterzik et al. (1995).
2. As discrimination parameter set we choose: *HR 1* and *HR 2* determined for each X-ray source, V of the closest optical counterpart in the GSC within $40''$ around the X-ray source, and the X-ray to optical flux ratio f_X/f_V . If no GSC counterpart is present within $40''$ we assign $V = 20$, thus allowing for the possible existence of a faint optical X-ray source not included in the GSC.
3. A k -nearest neighbourhood analysis is applied to all sources in the sample. A discrimination probability P_i for each source i is defined as

$$P_i = \frac{n(\text{TTS})}{k},$$
 where $n(\text{TTS})$ is the number of TTS in the training set “in the neighbourhood” of source i in the four dimensional discrimination parameter space. The neighbourhood is defined as the sphere containing exactly

$$n(\text{TTS}) + n(\text{non-TTS}) = k$$
 members of the training set. We have chosen $k = 20$. High values of P_i indicate that the source properties are similar to those within the sample of TTS of the training set.

Source selection on this basis implies a bias towards (X-ray and optical) properties of typical TTS in the training set, as desired. However, the selection cannot guarantee a “pure” TTS sample, because other classes of stars such as active binaries, RS CVn binaries, emission line dwarfs and some galaxies, share similar values within the discrimination parameter set, and are expected to contaminate any sub-sample.

The choice of the cutoff value for P_i is somewhat arbitrary. For our survey, we chose $P_i \geq 0.5$, resulting in a total of 170 WTTS candidates within our survey strip. Fig. 5 shows the surface density of rejected RASS sources near the Lupus region ($P_i < 0.5$) and the surface density of the RASS X-ray sources with $P_i \geq 0.5$.

3. Observations

Of the 170 selected RASS sources, 46 could be identified either from the SIMBAD database or from the previous study of Krautter et al. (1997). 115 more X-ray sources were observed at the ESO 1.52m-telescope with the Boller & Chivens spectrograph, the Loral CCD (ESO #39) and grating #5 in the nights of Apr 25, 96 to May 3, 96. The measured resolution (FWHM of unblended lines from the Helium-Argon calibration lamp) was 3.5 \AA for a slit width of $200 \mu\text{m}$ which was used for all program stars, and the spectral range was $4510 - 6780 \text{ \AA}$. Each night three spectrophotometric standard stars were observed.

Data reduction was performed using IRAF. The reduction consisted of bias subtraction, division by a flatfield, wavelength calibration, sky subtraction, extraction of the one-dimensional spectrum and flux calibration.

Spectral classification was accomplished by comparison with spectral standards from the MK catalog following the procedure outlined in Wichmann et al. (1996) for K and M stars. Although our setup favoured the red part of the spectrum, the good efficiency of the Loral CCD allowed us to use the line ratios $\text{CH } \lambda 4300/\text{Fe I } \lambda 4385$ and $\text{Fe I } \lambda 4385/\text{H } \gamma \lambda 4340$ recommended by Jaschek & Jaschek (1987) for the classification of F and G stars.

Fig. 1 summarizes the definition of the X-ray sample according to the discrimination probability P . We note that, above a discrimination threshold of 0.5, we have identified in total 161

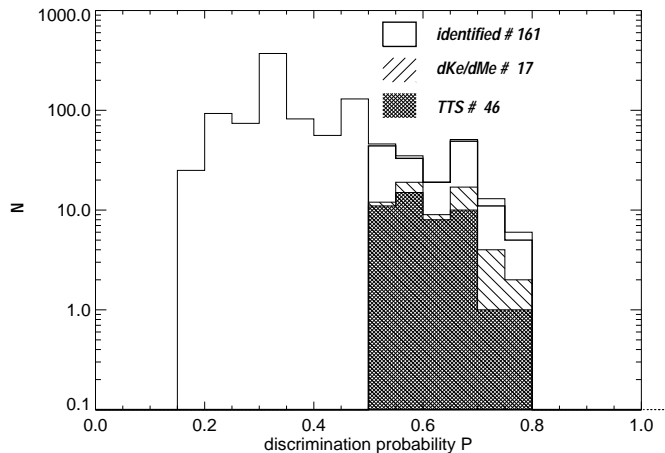


Fig. 1. Source selection: The histogram gives the distribution of discrimination probability P for all 1001 X-ray sources in our study area. Plotted is (on a logarithmic scale) the number of stars per P bin (with bin size 0.05). The thick line in the histogram indicates stars that have been identified (either observed or matched with known objects). The sub-sample of dKe/dMe stars is hatched and new PMS stars (including certain and possible new PMS stars) are cross-hatched. There are a total of 46 X-ray sources with counterparts classified as WTTS and 17 other X-ray sources with counterparts classified as dKe or dMe stars

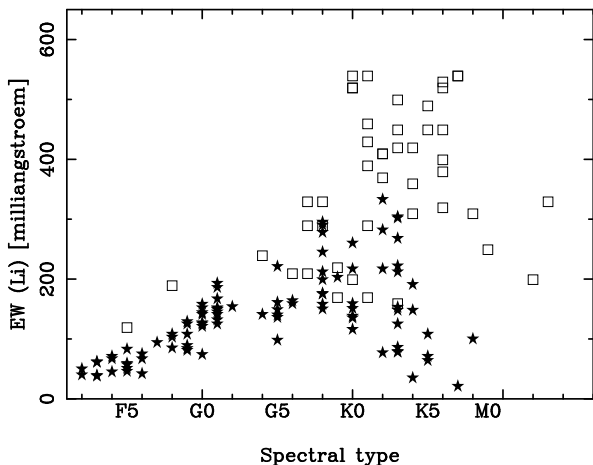


Fig. 2. Li I $\lambda 6708$ equivalent widths of WTTS found in our survey region (open boxes) as compared with Pleiades stars (stars). Data for Pleiades from Soderblom et al. (1993). Data for WTTS have been corrected for low dispersion as described in the text.

sources out of a total of 170 candidates, which implies a completeness of about 95%. The remaining nine sources were not observed due to lack of time.

4. Results

Of the 161 selected RASS X-ray sources either identified from catalogs or the previous study of Krautter et al. (1997), or studied in this work, 46 (29%) could be identified with WTTS on the basis of the presence of strong Li I $\lambda 6707$ absorption. In two

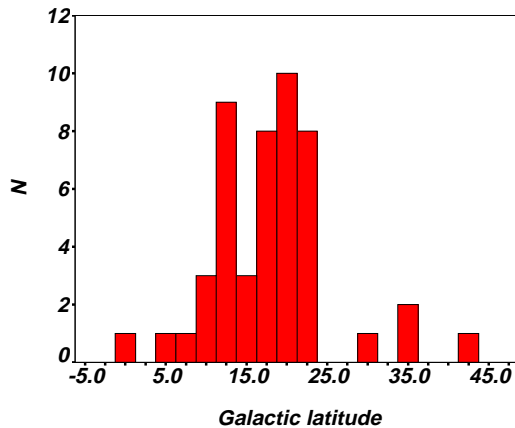


Fig. 3. Distribution of WTTS along galactic latitude within our survey strip.

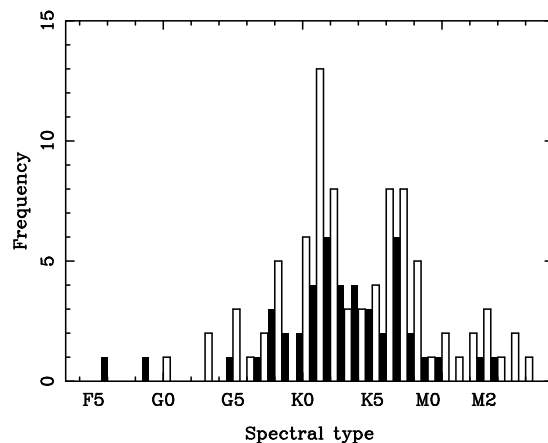


Fig. 4. Distribution of spectral types for dispersed WTTS near Lupus. Open bars: WTTS found by Krautter et al. (1997), filled bars (shifted to the right for 0.5 subclasses): this work.

cases two WTTS were found within the error circle of an X-ray source, thus yielding a total number of 48 WTTS for these 46 X-ray sources. These objects are listed in Table 1. The remaining 115 identified X-ray sources consist of galaxies (18), dMe/dKe stars (17), late-type main-sequence stars (67), and giants with spectral types earlier than K4 (13).

4.1. Lithium equivalent widths

In Fig. 2 we plot the Li I $\lambda 6707$ equivalent width $EW(\text{Li})$ of these WTTS against their spectral type, and also $EW(\text{Li})$ equivalent widths for the Pleiades sample from Soderblom et al. (1993). For the plot, we applied the following corrections to the $EW(\text{Li})$ values of our WTTS (as given in Table 1):

(i) At our resolution of 3.5 \AA , the Lithium line is blended with some nearby lines, which also might affect the determination of the continuum. Covino et al. (1997) have observed 27 WTTS of the Krautter et al. (1997) sample with CASPEC at the ESO 3.6 m telescope. Using their data, we computed the average off-

Table 1. WTTS identified with RASS X-ray sources within the region surveyed in this work. Designations are given in the standard notation for ROSAT X-ray sources. We list coordinates and visual magnitude m_V (both taken from the Hubble Guide Star Catalog), spectral type (this work), and Li I $\lambda 6708$ equivalent width EW(Li) for the WTTS counterparts. In addition, we list RASS X-ray countrate CR, Hardness ratios HR1/2 and the X-ray flux F_X , calculated according to the prescription given by Schmitt et al. (1995). For those WTTS that are common with Krautter et al. (1996), the designations are marked by the superior letter 'K'. Note: RXJ1512.8-4508A/B is a binary with ~ 6.1 arcsec separation.

No.	Designation	RA (2000.0)	Dec (2000.0)	Spectral type	m_V [mag]	EW(Li) [10 mÅ]	CR [1/sec]	HR1	HR2	$F_X/10^{12}$ [erg/cm ² /sec]
1	RXJ1410.8-2355	14:10:49.7	-23:55:28	K2	11.73	51	0.103	0.73	-0.28	1.25
2	RXJ1412.2-1630	14:12:14.1	-16:29:53	G9	11.43	31	0.047	0.80	0.09	0.59
3	RXJ1419.3-2322	14:19:21.1	-23:22:13	K0	9.58	34	0.083	0.93	0.38	1.10
4	RXJ1428.0-2927	14:28:02.0	-29:26:29	K6	13.76	59	0.046	1.00	-0.38	0.63
5	RXJ1447.3-3503	14:47:23.4	-35:03:13	K3	12.42	30	0.030	0.45	0.15	0.32
6	RXJ1448.2-4103	14:48:13.2	-41:02:59	K2	11.84	55	0.064	0.26	0.26	0.62
7	RXJ1450.4-3507	14:50:25.8	-35:06:48	K1	11.58	57	0.090	0.35	0.21	0.91
8	RXJ1450.5-3459	14:50:35.0	-34:59:05	K4	12.85	56	0.067	0.33	0.32	0.67
9	RXJ1452.4-3740	14:52:26.2	-37:40:09	K3	12.18	64	0.037	0.49	-0.26	0.40
10	RXJ1454.2-3955	14:54:11.2	-39:55:24	K2	12.32	55	0.043	0.47	-0.47	0.46
11	RXJ1455.8-3944	14:55:51.4	-39:43:46	F5	14.57	26	0.029	0.74	-0.11	0.35
12	RXJ1456.4-3947	14:56:25.7	-39:46:17	M2	14.65	47	0.037	0.57	0.43	0.42
13	RXJ1457.3-3613	14:57:19.6	-36:12:28	K7-M0	10.86	43	0.087	0.69	0.46	1.04
14	RXJ1458.6-3541	14:58:37.6	-35:40:30	K3	11.45	59	0.083	0.60	-0.44	0.95
15	RXJ1458.7-3315	14:58:45.8	-33:15:10	K1	11.83	53	0.049	1.00	-0.16	0.67
16	RXJ1459.3-4013	14:59:22.8	-40:13:12	G6	10.81	35	0.187	0.36	0.16	1.91
17	RXJ1500.6-4309	15:00:37.7	-43:08:34	K3	12.09	56	0.060	0.28	0.48	0.59
18	RXJ1500.8-4331	15:00:51.9	-43:31:21	K1	11.26	31	0.076	0.40	0.25	0.79
19	RXJ1501.2-4121	15:01:11.6	-41:20:40	G4	10.70	38	0.178	0.41	0.21	1.87
20	RXJ1502.4-3405	15:02:26.0	-34:05:12	K4	13.51	45	0.044	0.45	0.14	0.47
21	RXJ1504.8-3950	15:04:47.2	-39:49:25	F8	0.00	33	0.043	0.79	-0.35	0.54
22	RXJ1505.4-3857	15:05:25.9	-38:57:02	K6	12.55	52	0.073	0.65	-0.16	0.86
23	RXJ1505.4-3716	15:05:25.9	-37:15:33	M0	14.06	39	0.030	1.00	-0.10	0.41
24	RXJ1505.9-4312	15:05:56.9	-43:12:03	K7	13.35	68	0.049	0.38	0.28	0.51
25	RXJ1506.7-3047	15:06:42.6	-30:47:32	K7	13.97	68	0.021	1.00	0.63	0.29
26	RXJ1506.9-3714 ^K	15:06:54.3	-37:14:01	K0	14.50	68	0.048	0.76	0.80	0.59
27	RXJ1507.2-3505 ^K	15:07:14.8	-35:04:59	K0	11.24	66	0.074	0.72	0.26	0.90
28	RXJ1507.4-4601 ^K	15:07:27.5	-46:01:06	K1	11.71	43	0.065	0.44	0.51	0.69
29	RXJ1508.0-3338 ^K	15:08:05.1	-33:37:55	K6	13.08	46	0.057	1.00	0.06	0.78
30	RXJ1508.4-3338 ^K	15:08:25.0	-33:37:55	K7-M0	13.88	45	0.033	0.80	-0.61	0.41
31	RXJ1508.6-4423 ^K	15:08:37.8	-44:23:17	G8	11.28	47	0.173	0.46	0.20	1.86
32	RXJ1509.3-4420	15:09:17.7	-44:20:10	K4	11.23	50	0.028	1.00	-0.49	0.38
33	RXJ1511.0-3252 ^K	15:11:04.6	-32:51:30	K6	12.48	54	0.099	0.72	0.09	1.20
34	RXJ1511.6-3551 ^K	15:11:36.9	-35:50:41	K5	13.63	63	0.075	0.71	0.02	0.91
35	RXJ1511.6-3249A	15:11:36.7	-32:49:26	M1.5	15.03	34	0.052	1.00	-0.16	0.71
36	RXJ1511.6-3249B	15:11:39.6	-32:48:55	M1.5	15.06	34	0.052	1.00	-0.16	0.71
37	RXJ1512.6-3417	15:12:39.8	-34:16:59	K5	13.75	59	0.024	1.00	-0.63	0.33
38	RXJ1512.8-4508A	15:12:50.2	-45:08:04	G7	10.92	47	0.145	0.19	0.34	1.35
39	RXJ1512.8-4508B	15:12:50	-45:08:04	M1	16	47	0.145	0.19	0.34	1.35
40	RXJ1514.1-4104 ^K	15:14:07.5	-41:03:36	G7	10.84	35	0.074	0.48	-0.25	0.80
41	RXJ1514.7-4220 ^K	15:14:47.3	-42:20:15	K1	11.33	68	0.054	0.52	0.27	0.60
42	RXJ1515.7-3332 ^K	15:15:45.4	-33:31:59	K0	11.61	66	0.101	0.80	0.41	1.27
43	RXJ1515.8-4418 ^K	15:15:52.7	-44:18:17	K1	12.93	60	0.074	0.36	0.28	0.76
44	RXJ1518.0-4445	15:18:01.3	-44:44:26	K2	12.32	33	0.018	0.64	0.23	0.21
45	RXJ1519.6-4760	15:19:37.1	-47:59:34	G7	10.67	43	0.210	0.27	0.34	2.05
46	RXJ1529.8-4523 ^K	15:29:48.9	-45:22:45	K6	12.91	67	0.065	0.52	0.02	0.72
47	RXJ1534.6-4003 ^K	15:34:38.2	-40:02:28	K6	11.87	66	0.060	0.31	-0.28	0.60
48	RXJ1550.1-4746	15:50:12.0	-47:46:10	G9	11.59	36	0.035	0.98	0.07	0.47

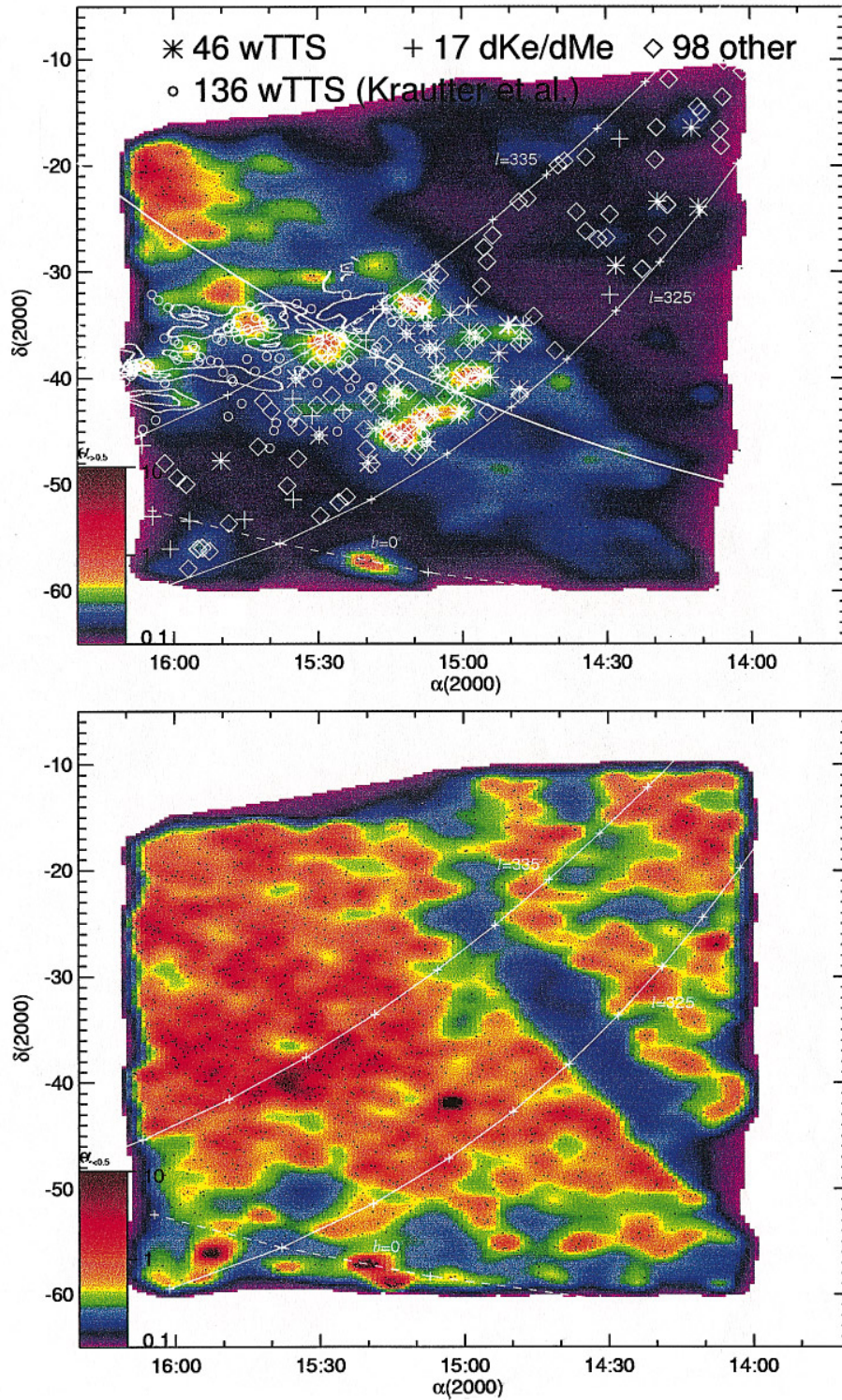


Fig. 5. Surface density plots (in units of $stars/deg^{-2}$) of WTTS candidate stars ($P_i \geq 0.5$, upper panel) and rejected RASS X-ray sources ($P_i < 0.5$, lower panel). For the definition of P_i see text (Sect. 2). The surface density is colour-coded with red showing the highest density (see scale on lower left in the plots). The position of the Lupus clouds is outlined by the CO map (white contours) from Murphy et al. (1986). The Gould Belt is indicated by a solid line in the upper panel.

set $O_{EW} = EW(Li, mid - resolution) - EW(Li, high - resolution)$. We derived a value of $O_{EW} \approx +140 m\text{\AA}$ at a spectral type of G0, decreasing to $O_{EW} \approx +60 m\text{\AA}$ at M5. However, as there is considerable scatter, this should only be regarded as a correction for the shift of the mean $EW(Li)$ at a given spectral type, while data for individual stars are quite uncertain.

(ii) As the $EW(Li)$ listed by Soderblom et al. (1993) already had been corrected for the contribution of the Fe I $\lambda 6707.44$ line, we also applied a correction for this line as given by Favata et al. (1993).

Typically the Li I $\lambda 6707$ equivalent width of our WTTS is significantly higher than that of Pleiades stars of the same spectral class. The small degree of overlap seen in Fig. 2 might be

attributable to the low precision of the Li equivalent widths measured on our medium-resolution spectra, or to strong intrinsic dispersion, which is also present in the Pleiades stars (Soderblom et al. 1993).

We conclude, that the WTTS found in our survey are most probably PMS stars rather than ZAMS stars like the Pleiades.

4.2. Spatial distribution

In Fig. 5, which displays the surface density of X-ray selected WTTS candidates, we can already see a 'ridge' of enhanced surface density that agrees well with the Gould Belt.

In Fig. 3 we show the distribution of the 48 spectroscopically identified WTTS along galactic latitude within the strip investigated, ranging from $b = -5^\circ$ to $b = +50^\circ$. Note that only one out of the 48 WTTS is located south of $b = +5^\circ$, which shows that these objects are completely unrelated to the Galactic Plane. Most of the objects are heaping in a region of about 15° width centered on $b \simeq +17.9^\circ$.

The most recent determination of the parameters of the Gould Belt was carried out by Comerón et al. (1994). On the basis of a catalog of 14,147 stars extracted from the INCA database (Gómez et al. 1989), they determined $i = 22.3^\circ$ for the tilt i to the Galactic Plane, and $\Omega = 284.5^\circ$ for the longitude Ω of the ascending node of the Gould Belt with respect to the Galactic Plane. At the central longitude of our strip ($l = 330^\circ$), this results in a latitude of $b = +15.9^\circ$ for the Gould Belt.

Comerón et al. (1994) do not give errors for their values of i and Ω , but typically errors of $2^\circ - 5^\circ$ for both parameters are quoted by other authors. Furthermore, the angular width of the Gould Belt is about $10^\circ - 15^\circ$. Thus we conclude, that the peak of the spatial distribution of dispersed WTTS found in our survey is in good agreement with the intersection of the plane of the Gould Belt and the strip investigated by us.

4.3. Comparison with previous work

In the study of Krautter et al. (1997), 86 WTTS have been found on the basis of RASS data near the Lupus dark clouds, dispersed over an area of some 230 square degrees. In Fig. 4 we compare the distribution of spectral types for our sample with that of the dispersed WTTS of Krautter et al. Apparently on average the WTTS found by Krautter et al. have a later spectral type than the WTTS of our sample.

However, this is easily explained by the fact that the survey of Krautter et al. was magnitude-limited with a limit of $m_V \lesssim 16$, while our survey was limited to RASS sources with GSC counterparts only. As the GSC contains only few stars with $m_V \lesssim 14$, with respect to the Krautter et al. survey we miss the fainter stars, i.e. those of late spectral type.

In order to compare both samples by a statistical test, we have to take into account the different magnitude-limits. We do this by considering only those 59 RASS-discovered WTTS of the Krautter et al. sample that are included in the GSC. For this sub-sample, we have compared the distribution of spectral types and magnitudes m_V with our sample of WTTS by means of a

two-sample Kolmogorov-Smirnov test. For the test hypothesis that both samples are drawn from the same parent population, we find a probability $p_{KS} = 83\%$ with respect to the distribution of spectral types, and $p_{KS} = 19\%$ with respect to the distribution of m_V (while for the rejection of the test hypothesis frequently limits of $p_{KS} \leq 5\%$ or even $p_{KS} \leq 1\%$ are used). We therefore conclude that with respect to the distribution of spectral types and m_V , the dispersed WTTS in our survey region near - but outside - the Lupus SFR are fully compatible with the dispersed WTTS found by Krautter et al. (1997) around the Lupus dark clouds.

5. Discussion

Our study region is located near to, but well outside the Lupus SFR, as defined by the Lupus dark clouds and the Lupus T Tauri associations near these dark clouds. As demonstrated in Sect. 4.3 the WTTS within our study region represent the same population of WTTS as the dispersed WTTS found by Krautter et al. (1997) around the Lupus dark clouds on the basis of RASS data. Therefore the conclusions drawn on the nature of the WTTS within our study region apply to both samples.

We have demonstrated in this work that within our study region the spatial distribution of WTTS along galactic latitude peaks at the intersection of the study region and the Gould Belt, while no concentration towards the galactic plane could be found. On the basis of this observation, we presume that the population of dispersed WTTS near Lupus forms part of the Gould Belt, like the Lupus SFR. Thus, the age of these stars is limited by the age of the Gould Belt, i.e. some $50 - 60 \times 10^6$ yrs, and their distance towards us probably is not much different from the distance of the Lupus SFR.

It remains unclear whether these stars originate in the Lupus dark clouds, or whether they have formed in smaller cloudlets which have dispersed since, as suggested by Feigelson (1996). In any case, it seems highly unlikely that they represent a galactic foreground population of 10^8 yrs old ZAMS stars, as proposed by Briceño et al. (1997). Thus, our results represent an independent confirmation of the conclusions of Krautter et al. (1997) and Wichmann et al. (1996) on the PMS nature and the youth of the dispersed WTTS found by them.

Acknowledgements. We are very grateful to Drs. Covino and Alcalá for discussions. This research was supported by grant KR 1053/3 from the DFG, Germany, and grant 50OR90017 (Verbundforschung Astronomie) from the BMFT, Germany. The ROSAT project is supported by the Bundesministerium für Bildung, Wissenschaft, Forschung und Technologie (BMBF/DARA) and the Max-Planck-Gesellschaft. This research has made use of the SIMBAD database, operated at CDS, Strasbourg, France.

References

- Alcalá J.M., Krautter J., Schmitt J.H.M.M. et al. 1995, A&AS 114, 109
- Briceño C., Hartmann L.W., Stauffer J.R. et al. 1997, ApJ, in press
- Comerón F., Torra J. 1990, A&A 241, 57
- Comerón F., Torra J., Gómez A.E. 1994, A&A 286, 789
- Covino, E. et al. 1997, A&A in preparation

- Dubath P., Reipurth B., Mayor M. 1996, A&A 308, 107
Favata F., Barbera M., Micela G., Sciortino S. 1993, A&A 277, 428
Feigelson E.D. 1996, ApJ 468, 306
Frogel J.A., Stothers R. 1977, AJ 82, 890
Gómez A.E., Morin D., Arenou F. 1989, in: The Hipparcos Mission, vol. II, eds. M.A.C. Perryman & C. Turon, ESA SP-1111
Gould B.A. 1879, in: Uranometria Argentina, ed. P.E. Corni, Buenos Aires, p. 355
Jaschek C., Jaschek M. 1987, The classification of stars, Cambridge University Press, Cambridge
Jones B.F., Herbig G.H. 1979, AJ 84, 1872
Krautter J., Wichmann, R., Schmitt et al. 1997, A&AS 123, 329
Murphy D.C., Cohen R., May J. 1986, A&A 167, 234
Neuhäuser, R., Sterzik, M.F., Torres, G., Martin, E.L. 1995, A&A 299, L13
Olano C.A. 1982, A&A 112, 195
Pöppel W.G.L., Marronetti P., Benaglia P. 1994, A&A 287, 601
Soderblom D.R., Jones, B.F., Balachandran, S., et al. 1993, AJ 106, 1059
Sterzik M.F., Durisen R. 1995, A&A 304, L9
Sterzik M.F., Alcalá J.M., Neuhäuser R., Schmitt J.H.M.M. 1995, A&A 297, 418
Stothers R., Frogel J.A., 1974, AJ 79, 456
Westin, T.N.G. 1985, A&AS 60, 99
Wichmann, R., Krautter, J., Schmitt, J.H.M.M. et al. 1996, A&A 312, 439